Online Appendix for: "*Enforcement Policy in a Dynamic Model of Deterrence*"

Clifford Bekar* Kenneth I. Carlaw† B. Curtis Eaton‡

Revised January 10, 2024

*Associate Professor, Economics, Lewis and Clark College, bekar@lclark.edu.

†Professor, Economics, University of British Columbia - Okanagan, kenneth.carlaw@ubc.ca.

‡Emeritus Professor, Economics, University of Calgary and Honorary Professor, Economics, University of British Columbia - Okanagan, eaton@ucalgary.ca.

Contents

1 Road map to the appendix

This appendix provides empirical evidence, robustness testing, technical descriptions of the computational tools developed, and a guide to codebases that replicate figures in support of *"Enforcement Policy in a Dynamic Model of Deterrence"*. Links to the relevant code bases are provided where simulations are discussed.

Section 2 presents data and empirical analysis of data on crime and related indicators. The empirical literature relating to the two empirical signatures provided in Proposition 2 of Sah (1991) is first reviewed. Then empirical evidence of those signatures in the US and Canadian crime data is presented in the form of autocorrelations and serial correlations from the raw data and some simple regression analysis. Section 3 provides the set of robustness test conducted on the model's key assumptions and core parameters. Several composite parameters are defined and analyzed. The space of history independent policies is generalized in the parameter F. Detailed results on history dependent policies are provided and some general features of those policies are explored. Section 4 provides the technical descriptions of several computational tools developed to produce the simulation results for the main paper and for Section 3. Section 5 provides the code bases for all of the figures presented in the main text. Section 6 provides technical details on Pareto-dominant equilibria for the S-Model.

We have implemented most of our numerical simulations in two wholly separate codebases, *Matlab* and *Python.* Our reported results have been independently replicated in each codebase. One member of our team wrote and maintained the Matlab codebase, another wrote and maintained the Python codebase.

All code can be found at the following Github repository:

- Links to online appendix: All materials, Python Codebase, Matlab Codebase

2 Evidence that deterrence is a dynamic process

This section presents empirical evidence supporting Bentham's and Sah's views that deterrence is a dynamic process. We first present evidence from three bodies of literature on deterrence. We then analyze U.S. and Canadian crime rate and economic opportunities data to present additional evidence.

2.1 Empirical signatures of a dynamic deterrence process

In his Proposition 2, Sah (1991, p. 1282) identifies two empirical signatures of dynamic deterrence processes. Positive autocorrelation in the number of crimes committed is the first signature—"Past crime breeds future crime. That is, the current crime participation rate is higher if the crime participation rate was higher in a past period." A negative correlation between crimes committed in a period and the quantity of deterrence resources in a previous period is the second signature—"The current crime participation rate is also higher if fewer resources were spent on the criminal apprehension system in a past period...". These signatures are incompatible with static models of deterrence but are inescapable attributes of dynamic models in which the subjective probabilities are historically determined.

Regarding positive autocorrelation, Jacob et al. (2007, p. 89-90) point out that "The persistence of criminal activity is well documented. Higher crime today in any particular area is associated with higher crime tomorrow...A 10 percent increase in violent crime in a typical city this week is associated with 1.6 percent more violence the following week, conditional on jurisdiction-year fixed effects. The serial correlation for property crime is even higher—10 percent more property crime this week is associated with over 3.1 percent more property crime the following week."[1]

The divergence between the predictions of static models of deterrence and the data has

[1] Worrall and Pratt (2004, p. 37) note the widespread autocorrelation in crime data which is rarely "independent along the time dimension. We expect serial dependence (often referred to as serial autocorrelation and/or temporal autocorrelation)." In their econometric analysis all significant coefficients on lagged crime are positive (Worrall and Pratt, 2004, see Tables 1 and 2 on pp. 42, 44).

resulted in a large and active literature attempting to locate the exogenous source of the observed autocorrelation and crime waves.[2] Potential explanations include business cycle effects, weather, and changes in the supply of certain illegal narcotics..[3] That no single explanation has emerged suggests that the persistence of crime, and the emergence of crime waves, are to be understood as consequences of a dynamic process.

Fajnzylber et al. (1998) explicitly test Sah's Proposition 2 using international data that covers most of the countries in the world.[4] Their empirical findings include: (i) their static deterrence model is misspecified;[5] and, (ii) lagged crime is an important correlate of contemporaneous crime.[6] They summarize their findings by arguing that their "empirical findings regarding criminal inertia imply that current crime rates respond to current policy variables with a lag" (Fajnzylber et al., 1998, p. 31). They anticipate our analysis of history dependent policy in Section 4.3 of the paper, arguing that the existence of "criminal inertia" implies that when confronted with rising crime "policy-makers should act to counter the crime wave, if not, a country may get stuck at an excessively high crime rate" (Fajnzylber et al., 1998, p. 31).

Corman and Mocan (2000) analyze the impact of drug use and policing on crime using 30 years of high frequency monthly data from New York city. They provide extensive evidence supporting both elements of Sah's Proposition 2. Their Tables 2 and 3 report that rates of murder, assault, robbery, and burglary are all determined in part by lagged crime rates, arrest rates, and policing resources.[7] They argue that these lagged effects are not due

[2] Jacob et al. (2007, p, 491) argue that static models of deterrence cannot account for the observed persistence, "Beginning with Becker (1968), economic models of criminal behavior have generally been constructed and tested using a static framework. While these models have been very useful in understanding some features of criminal behavior, they are not well suited to explaining how criminal behavior changes over time."

[3] See, for example, Curry et al. (2016), Glaeser et al. (1996), Greenberg (2017), Loureiro (2013), and Mocan and Bali (2010).

[4] See also Fajnzylber et al. (2002).

[5] See Tables 2 and 3 for their static specification for homicide and robbery, Tables 4 and 5 for the dynamic specification. In both cases they find "The model specification without a lagged dependent variable...is strongly rejected..." (Fajnzylber et al., 1998, p. 29).

[6] See their Tables 4 and 5 where the coefficients on both lagged homicide and robbery are both significant and positive. They are roughly the same size as we report in Table 5 below.

[7] Their use of high frequency data allow Corman and Mocan (2000) to test a range of complex lag

to incapacitation, but, likely, persistence of subjective probabilities, "It is plausible that increased arrests do not immediately affect criminal behavior. It takes time for criminals and potential criminals to perceive that such a change has occurred. To the extent that it takes at least a month for criminals to process that information and to change their behavior, crime should depend on lagged arrests" (Corman and Mocan, 2000, p. 592).

There is substantial additional empirical evidence regarding the second signature.[8] Lim and Galster (2009, p. 943) develop a theoretical model "wherein benefits and costs of property crime are endogenous to neighborhood property crime rates lagged over two periods." They then show that policy effects display various lags, but that jurisdictions return to their steady state levels of crime within 10 years. Loureiro (2013, p. 2) models hystersis in crime, which "can be understood as a path-dependent process, where the current level of crime depends not only on the current levels of variables like the number of police officers and income, but also whether their levels in the previous periods were below or above the current levels." The focus of Loureiro (2013) is how such lags produce hysteresis and, ultimately, nonlineraties in deterrence policy. For example, these "asymmetric effects are also observed for positive and negative variations in the number of police officers for all crime rates, except larceny and rape. Reductions of one standard deviation in the size of the police force increase those crime rates by one to four standard deviations" while the effect of increases in the police force are 'significantly smaller' depending on the types of crime" (Loureiro, 2013, p. 36).

A common finding in the perceptions literature is that the most reliable predictors of subjective probabilities are local and/or personal histories.[9] In his review Apel (2013, p. 84) finds that "While cross-sectional research on the strength of the correlation between objec-

structures, which may differ by variable analyzed and type of crime. The authors also provide evidence for autocorrelation in crime in Corman and Mocan (2005).

[8] Lochner (2007, p. 444) argues that his empirical findings regarding subjective probabilities supports Sah's Proposition that "when the probability of arrest is learned from others or through one's own experiences, the effects of policy tend to be lagged and long-lasting."

[9] Two approaches dominate the perceptions literature: (i) survey methods, do people report accurate knowledge of the size and probability of sanction; and, (ii) revealed behavior, do populations respond as if they have accurate knowledge of the size and probability of sanction?

tive sanctions and risk perceptions...has revealed that individuals are typically poor judges of the certainty and severity of punishment (or at least imperfect estimates thereof), panel research on the experiential component of the perceptual deterrence model has revealed that personal experiences and, to a lesser degree, vicarious experiences with crime and punishment are salient determinants of changes in risk perceptions." He goes on to note that "A number of studies provide support for the Bayesian updating model with respect to crime and punishment experiences...Put simply, offenders update their subjective probabilities of arrest risk upward as a result of sanctioned offending, but update them downward as a result of unsanctioned offending" (Apel, 2013, p. 85).

Lochner (2007, p. 444) finds evidence that subjective probabilities of apprehension evolve with the history of the system and specifically that one's own experience and that of others whom they know are important determinants of those probabilities. He notes that "Individuals who engage in crime while avoiding arrest tend to reduce their probability of arrest; those who are arrested raise their perceived probability. Beliefs respond similarly to changes in the criminal history of their siblings, but they do not appear to adjust in response to a sibling's arrest. Thus, individuals may share information and learn from other family members, but the evidence on this is mixed" (Lochner, 2007, p. 457-58).[10]

Two key aspects of dynamic deterrence policy—the determinants of subjective probabilities and the lagged effect of policy—intersect in what are known as crackdowns, hotspot policing, or what we call history dependent policies. Crackdowns are policies that rely on a short lived increase in deterrent resources in a jurisdiction that produce a durable reduction in crime.[11] Sherman (1990, p. 10) argues that the effect of crackdowns persists because the "perceived risk of apprehension could influence decisions not to commit offenses after the risk (or the communicated threat) is actually reduced, at least until such time as other evidence shows the quasi-rational actors that the risk has returned to its prior level." An

[10] Matsueda et al. (2006) finds evidence both that subjective and objective probabilities differ and that people update as Bayesians.

[11] See, for example, Banerjee et al. (2019), Hansen (2015), Weisburd (2021), Perc et al. (2013), Fu and Wolpin (2018), Ratcliffe et al. (2015), and Poutvaara and Priks (2006).

empirical analysis of crackdowns finds that "risk perceptions may decay only slowly, even when the actual police effort has been returned to normal" (Sherman, 1990, p. 3).[12] This renders crackdowns durable, so that "By constantly changing crackdown targets, police may reduce crime more through residual deterrence than through initial deterrence."[13]

2.2 Dynamic signatures in US and Canadian crime data

To illustrate how prominent the empirical signatures identified by Sah (1991) are in crime data, we use annual data on crimes committed and the number of enforcement employees (in both cases expressed as a rate per 100,000 people) for the 50 United Sates and the District of Columbia for the years 1985-2021, and for 10 Canadian provinces for the years 1999-2020. The data sources are the Federal Bureau of Investigation's Crime Data Explorer and Statistics Canada's Incident Based Crime Statistics.

Tables 1 and 2 show that the evidence for the first signature—positive autocorrelation in the time series of the crime rate—is quite strong in the raw data. For example, in the U.S., with one exception, the correlation coefficients between the crime rate in year t and that in years $t-1$, $t-2$ and $t-3$ are positive in all 51 jurisdictions for all three lags, and they tend to be large. For a one year lag the correlation coefficients in 35 states exceed 0.9, and they exceed 0.8 in 48 states. In every jurisdiction the coefficients decrease with longer lags, but even at 3 years the coefficients are relatively large with 48 of them exceeding 0.6 and 37 exceeding 0.7.

On the second signature—Tables 3 and 4 show a negative relationship between the crime rate in year t and enforcement resources in previous years—the evidence in the raw data is

[12] Banerjee et al. (2019) model how learning about the pattern of crackdown deployments might endogenously determine violation strategies. Their empirical findings overlap with ours in potentially interesting ways. Specifically, they find that crackdowns produce residual deterrence by altering people's subjective apprehension risk and that "when we alter our assumptions to require citizens' beliefs about police activity to be correct in expectation, we find that the optimal police strategy becomes one of a short, intense crackdown mostly done in one location" (p. 44).

[13] The evidence for crackdowns rests largely, although not exclusively, on the qualitative analysis of case studies. Sherman (1990, p. 35-6) finds durable reductions in crime for 13 of the 15 cases he analyzes. For a review of dynamic policing policies see Chalfin and McCrary (2017, pp. 17 - 24) and Nagin (2013), especially Section 4.2, and MacDonald et al. (2016).

Table 1: Autocorrelation of crime (US states, 1985-2021).

	Lagged crime rates				Lagged crime rates		
State	**1 lag**	**2 lags**	**3 lags**	**State**	**1 lag**	**2 lags**	**3 lags**
AL	0.9004	0.7416	0.5766	MT	0.8619	0.7163	0.6038
AK	0.8518	0.6455	0.3309	NE	0.8580	0.6974	0.5155
AZ	0.9298	0.8316	0.7450	NV	0.7358	0.4067	0.0974
AR	0.7078	0.4593	0.2228	NH	0.7955	0.6407	0.5062
CA	0.9655	0.9033	0.8260	NJ	0.9439	0.8745	0.7965
CO	0.9189	0.7897	0.6430	NM	0.8646	0.6909	0.5036
CT	0.9306	0.8371	0.7454	NY	0.9618	0.8993	0.8173
DE	0.8256	0.6577	0.4386	NC	0.9511	0.8682	0.7600
DC	0.9302	0.8239	0.6929	ND	0.9061	0.8242	0.7423
FL	0.9514	0.8892	0.8125	OH	0.9378	0.8455	0.7363
GA	0.9530	0.8700	0.7674	OK	0.8877	0.7139	0.5059
HI	0.1975	0.0476	-0.1575	OR	0.9452	0.8800	0.8085
ID	0.7784	0.6328	0.5143	PA	0.8498	0.6956	0.5765
IL	0.9591	0.8961	0.8275	RI	0.9198	0.8548	0.7782
IN	0.9054	0.7356	0.5366	SC	0.9383	0.8505	0.7474
IA	0.4974	0.3948	0.1860	SD	0.8286	0.7488	0.6477
KS	0.7677	0.4733	0.1455	TN	0.7995	0.6076	0.4188
KY	0.9102	0.7788	0.6229	TX	0.9408	0.8485	0.7438
LA	0.9335	0.8375	0.7031	UT	0.9022	0.7647	0.6252
ME	0.7318	0.6719	0.5403	VT	0.7702	0.4618	0.1806
MD	0.9311	0.8597	0.7885	VA	0.9501	0.8786	0.7894
MA	0.9290	0.8435	0.7451	WA	0.9532	0.8922	0.8231
MI	0.9340	0.8375	0.7610	WV	0.8550	0.7128	0.6136
MN	0.9085	0.7697	0.6151	WI	0.6807	0.4681	0.3658
MS	0.9203	0.8009	0.6454	WY	0.7688	0.6408	0.4871
MO	0.8980	0.7440	0.5966				

Table 2: Autocorrelation of crime (CDN provinces, 1999-2020).

	Lagged policing resources (1)	(2)	(3)
Province	**1 lag**	**2 lags**	**3 lags**
NL	0.6065	0.3016	0.0607
PEI	0.8656	0.6715	0.5324
NB	0.8465	0.6682	0.4827
NS	0.9097	0.7904	0.6832
QE	0.8751	0.7619	0.6495
ON	0.8530	0.7353	0.6251
MN	0.8826	0.7507	0.6186
SK	0.8775	0.7309	0.5895
AL	0.8083	0.5899	0.4159
BC	0.8943	0.7925	0.7160

Table 3: Serial correlation of crime on policing (US states, 1985-2021).

	Lagged policing resources				Lagged policing resources		
State	**1 lag**	**2 lags**	**3 lags**	**State**	**1 lag**	**2 lags**	**3 lags**
AL	-0.5037	-0.4815	-0.5890	MT	-0.7394	-0.7094	-0.6971
AK	-0.0925	-0.2474	-0.3099	NE	-0.6263	-0.6746	-0.7143
AZ	0.4066	0.3762	0.3761	NV	0.7254	0.6878	0.6607
AR	-0.6196	-0.6853	-0.7256	NH	-0.4296	-0.4282	-0.4345
CA	-0.4231	-0.4668	-0.5279	NJ	-0.1690	-0.0538	-0.0637
CO	0.0995	0.0584	0.0079	NM	-0.2783	-0.4779	-0.5886
CT	0.7422	0.7103	0.6614	NY	-0.3107	-0.3310	-0.3524
DE	0.3070	0.2898	0.2935	NC	-0.3217	-0.4521	-0.5632
DC	0.2370	0.1907	0.1227	ND	-0.5349	-0.5581	-0.5429
FL	-0.2477	-0.2956	-0.4383	OH	-0.7487	-0.7159	-0.6708
GA	-0.0053	-0.0520	-0.1388	OK	-0.6134	-0.6136	-0.5808
HI	0.4231	0.4054	0.3566	OR	-0.1400	-0.1500	-0.1603
ID	0.6057	0.6418	0.6639	PA	0.1120	-0.0420	-0.1684
IL	-0.6198	-0.6167	-0.6147	RI	-0.6135	-0.6086	-0.5772
IN	-0.8648	-0.8989	-0.9163	SC	-0.4784	-0.5614	-0.5938
IA	-0.7039	-0.7266	-0.7374	SD	-0.6649	-0.6668	-0.6663
KS	-0.6725	-0.7074	-0.7326	TN	-0.4090	-0.4538	-0.4759
KY	-0.5811	-0.6227	-0.6319	TX	-0.2300	-0.3193	-0.3074
LA	-0.6145	-0.6723	-0.7566	UT	0.1693	0.1249	0.0641
ME	-0.8339	-0.8556	-0.8123	VT	-0.4667	-0.4646	-0.4222
MD	-0.5174	-0.5747	-0.6215	VA	-0.7289	-0.7635	-0.7932
MA	-0.6238	-0.6246	-0.6001	WA	0.3530	0.2962	0.2405
MI	0.7546	0.7378	0.7130	WV	-0.3404	-0.3435	-0.3632
MN	-0.7286	-0.7413	-0.7431	WI	-0.2898	-0.2864	-0.3432
MS	-0.4753	-0.5535	-0.6212	WY	0.0655	0.05607	0.1945
MO	-0.8247	-0.8645	-0.8803				
				negative	**38**	**39**	**39**

not as strong as it is for the first, but it is there. For example, in 38 to 39 of the 51 U.S. jurisdictions the correlation coefficients between the crime rate in year t and enforcement resources in years $t-1$, $t-2$ and $t-3$ are negative for all three lags. But in the other 12 they are positive for all 3 lags.

To get a better sense for the economic and statistical significance of these relationships, we pooled the data and ran regressions with the crime rate in period t as the dependent variable. We controlled for differences across US states and Canadian provinces using state/province fixed effects. We also controlled for variation in the unemployment rate and average personal income.[14] The explanatory variables of interest are the lagged values of the crime rate and

[14] The US unemployment data are obtained from the Federal Reserve of St. Louis FRED database, and US the Personal Income data is obtained from Bureau of Economic Analysis database table SAINC1: State Annual Personal Income Survey. The Canadian unemployment data and household income data are from the Statistics Canada's Labour Force Characteristics by Industry and Distributions of Household Economic Accounts tables. The estimated coefficients on the controls have signs consistent with predicted values - positive for unemployment rates and negative for personal income. The estimated coefficient on personal income is highly significant while that for unemployment is not significant. Unemployment rates and personal

Table 4: Serial correlation of crime on policing (CDN provinces, 1999-2020).

	Lagged policing resources		
	(1)	(2)	(3)
Province	**1 lag**	**2 lags**	**3 lags**
NL	0.3011	0.1366	-0.0131
PEI	0.2599	0.1209	-0.0696
NB	-0.0169	-0.1960	-0.3354
NS	-0.6996	-0.7716	-0.8407
QE	0.2145	0.1030	-0.0758
ON	-0.0225	-0.1591	-0.3070
MN	-0.4033	-0.6495	-0.7543
SK	-0.2348	-0.4459	-0.6042
AL	-0.6969	-0.7567	-0.7539
BC	-0.6105	-0.7227	-0.8180
negative	**7**	**7**	**10**

enforcement resources. The times series for both are highly collinear, so it is difficult to accurately estimate the independent effects for different lags. For this reason, we include just one lagged value of the crime rate and enforcement resources in our regressions. In Table 5 we report results for the regressors of interest when the lag is one period.

income exhibit co-linearity in our regression model. We did not control for demographic effects on the crime rate because we could not find data that was consistent over time and across jurisdictions.

Table 5: Regression analysis: Crime rates.

Panel A: US states, 1985-2021	(1)	(2)
Model	FE	FE
Options	OLS	robust
No. Obs	(1785)	(1785)
Lagged crime rate	0.91***	0.92***
	(0.01)	(0.01)
Lagged policing	-0.67***	-1.08***
	(0.23)	(0.22)
Controls	yes	yes
R-squared	0.97	0.98
Panel B: Canadian provinces, 1999-2000	**(1)**	**(2)**
Model	FE	FE
Options	OLS	robust
No. Obs	(230)	(230)
Lagged crime rate	0.84***	0.85***
	(0.03)	(0.03)
Lagged policing	-1.26***	-1.27***
	(0.32)	(0.31)
Controls	yes	yes
R-squared	0.98	0.98

Standard errors are in parentheses.
Significant at the *** 1% level.

The point estimates are economically significant—a 1% increase in the crime rate in period $t-1$ induces an increase in the period t crime rate of approximately 0.9%, and 1% increase in enforcement resources induces a decrease in the crime rate of approximately 0.67% using the OLS estimate and 1.08% using the robust estimate. The estimates are statistically significant. The point estimates for the lagged crime rate are 90 times their standard errors, while the point estimates for lagged enforcement resources are 3 to 5 times their standard errors.

3 Robustness

In this section we layout a series of robustness tests, demonstrating that the D-model's central results are robust to a range of alternative specifications and variations on the the baseline parameterization.

3.1 General nature of positive feedback (CLIFFSET and DROP)

As we have seen, the D-model produces a suite of features including the *cliff of expected violations*.

(i) As R increases from 0 one can distinguish three regimes: initially there is an unruly regime where $E(v|R)$ is relatively high and slowly decreasing in R, followed by a transitional regime in which $E(v|R)$ drops precipitously as R increases, and finally a compliant regime where $E(v|R)$ is relatively low and virtually constant.

(ii) There is a single q-attractor in the unruly and compliant regimes. In the unruly regime the number of violations at the focal point of the q-attractor BA is relatively high and decreases slowly with R; in the compliant regime the focal point of the q-attractor GA is relatively low and unresponsive to R.

(iii) There are two q-attractors in the transitional regime: GA where the focal point violations are low and BA where the focal point violations are high. As R transits between the unruly and compliant regimes, the persistence of BA diminishes from approximately 1 to roughly 0 while the persistence of GA increases from approximately 0 to roughly 1.

(iv) Items (ii) and (iii) produce a prominent cliff-like structure in the relationship between the quantity of enforcement resources R and the expected number of violations in the stationary distribution $E(v|R)$.

(v) In all three regimes there is significant positive autocorrelation in the time series of violations for lags of one, two and three periods and for much longer lags in the transitional regime.

We develop a measure of the prominence of the cliff called $DROP$. Prominent cliffs produce large values of $DROP$, inconspicuous cliffs produce low values of $DROP$. We then define $CLIFFSET$ as the set of parameterizations such that $DROP$ exceeds a threshold

value. In subsequent sections we report evidence that DROP itself is an economically interesting statistic.

The geometric signature of the cliff is a small range of contiguous values of R such that as R is increased through that range there is a dramatic drop in $E(v|R)$. We set the range of R to $RANGE = INT(0.05 \cdot N)$. For the baseline parameterization $RANGE = 5$.

For a given a parameterization we first estimate the relationship $E(v|R)$ for all $R \in \{0, ..., N\}$. For every integer $X \in \{0, ..., N - RANGE)$ we then calculate the reduction in $E(v|R)$ when R is increased from X to $X + RANGE$. $DROP$ is the maximum value of this difference normalized as a fraction of its maximum possible value, N.

$$DROP = \frac{\max_{\{X\}}[E(v|R = X) - E(v|R = X + RANGE)]}{N}$$

Intuitively, $DROP$ measures the height of the cliff relative to the size of the population of potential violators. It is bounded below by 0 and above by 1. For example, $DROP = 0.5$ indicates that in the vicinity of the cliff an increase of $INT(0.05 \cdot N)$ in R reduces the expected number of violations in the stationary distribution by $0.5 \cdot N$, or that the slope of the cliff is approximately -10. In defining $CLIFFSET$, we set the threshold value of $DROP$ to 0.35, producing a slope of -7. The value of $DROP$ for the baseline parameterization is roughly 0.7, producing a cliff with a slope of -14.

Figure 1 plots three different cliffs: one for the baseline parameterization, one in which $DROP = 0.35$, and in which $DROP = 0.1$. The baseline produces the most prominent cliff and the largest value of DROP.

The code that produces Figure 1 can be found here:

- Matlab file(s): Figure 3

$DROP$ is a function of six parameters, $\mu, \sigma, \gamma, F, N$ and z, so $CLIFFSET$ is an object

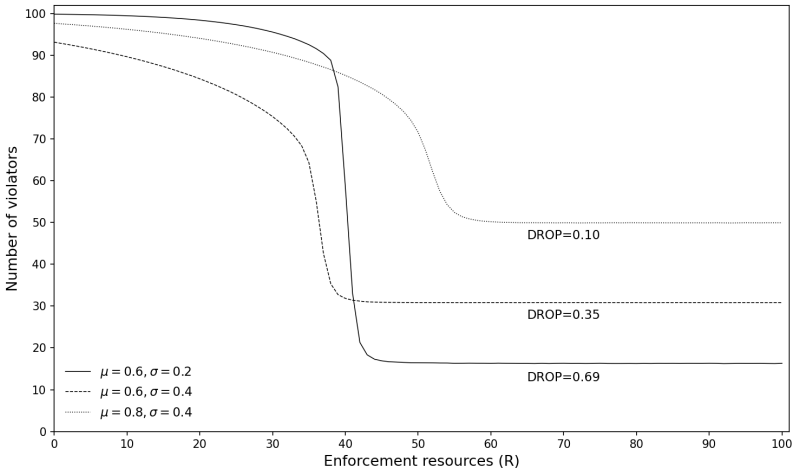

Figure 1: Three cliffs of expected violations and their measured $DROP$.

in a six dimensional space.

$$CLIFFSET = \{\mu, \sigma, \gamma, F, N, z | DROP \geq 0.35\}$$

While a complete description is not feasible, we can describe some of the most important aspects of $CLIFFSET$. Since the underlying behavior of the model depends only on the value of $\gamma \cdot F$, and not independently on γ or F, we are able to reduce $CLIFFSET$'s dimensionality by treating $\gamma \cdot F$ as a composite parameter. Think of $\gamma \cdot F$ as the size of the deterrence stick. We start by describing a subset of $CLIFFSET$,

$$CLIFFSET' = \{\mu, \sigma \ | DROP \geq 0.35, \ \gamma \cdot F = 0.80, \ N = 100, \ z = 2\}$$

In Figure 2, we have constructed a surface plot of $DROP$ for $\mu \in \{0, 0.05, 0.1, ..., 1.00\}$ and $\sigma \in \{0.15, 0.20, ..., 0.55\}$ (so the set of (μ, σ) pairs has 189 elements).[15] We have included a shaded reference plane representing our threshold value of $DROP$. The outer boundary of $CLIFFSET'$ is defined by the locus of points where the surface plot and the reference plane intersect. We have projected the iso-DROP locus for $DROP = 0.35$ onto the baseplane,

[15] We have not included estimates of DROP for values of σ less than 0.10 because our convergence simulation routine is not reliable for small values of σ.

$CLIFFSET'$ is the set of (μ, σ) pairs on and inside the iso-DROP locus.

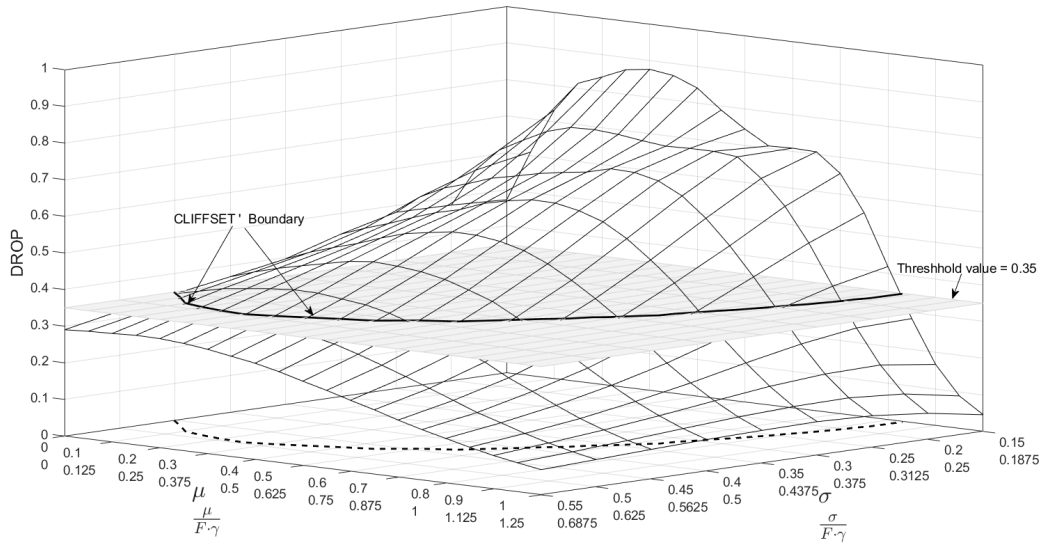

Figure 2: $DROP$ for a range of μ and σ.

The code that produces Figure 2 can be found here:

- Matlab file(s): Figure 4

There is another interpretation of $CLIFFSET'$. Setting $s > 0$ and applying this scalar to three key parameters of $CLIFFSET'$, $(s \cdot \mu, s \cdot \sigma, s \cdot \gamma \cdot F)$, the ratio of the new set of values for $DROP'$ and the original $DROP$ values are, to a very close approximation, equal to 1. In other words, $DROP$ is homogeneous of degree 0 in μ, σ and $\gamma \cdot F$. This follows from the fact that the probability π that any person chooses violate in any period is homogeneous of degree 0 in these same parameters. In every period, every person has a well defined subjective probability of apprehension, q. When their opportunity g is revealed they choose violate if and only if $g > q \cdot \gamma \cdot F$. Prior to the realization of g, the probability π that they choose violate is $1 - \Phi(q \cdot \gamma \cdot F)$. Since $\phi(g)$ is normal, $\Phi(q \cdot \gamma \cdot F)$ and hence π, are themselves $HD0$ in μ, σ and $\gamma \cdot F$.

Proposition 1 *Given any parameterization of the model* $(\widehat{\mu}, \widehat{\sigma}, \widehat{\gamma} \cdot \widehat{F}, \widehat{z}, \widehat{N}, \widehat{R})$ *and the constructed parameterization* $(s \cdot \widehat{\mu}, s \cdot \widehat{\sigma}, s \cdot \widehat{\gamma} \cdot \widehat{F}, \widehat{z}, \widehat{N}, \widehat{R})$*, where* $s > 0$*, the expected choices of potential violators are identical.*

In light of proposition 1 a simple rescaling of the μ and σ axes and a redefinition of the variables the axes represent allows us to reinterpret Figure 2. The surface plot in the figure represents the DROP statistics for pairs $(\frac{\mu}{\gamma \cdot F}, \frac{\sigma}{\gamma \cdot F})$, and the set identifies the subset of $CLIFFSET$ for any parameterization in which $N = 100$ and $z = 2$.

$DROP$ is increasing in both N and z, and hence for larger values of either or both of these parameters the associated subset of $CLIFFSET$ is somewhat larger than the one identified in Figure 2. To give a sense of how sensitive the subset is to these variables we have calculated DROP statistics for $z = 3$ and for $N = 160$ for three points on the outer boundary of $CLIFFSET'$.

Table 6: DROP statistic for N=160 and z=3.

Threshold tuples $(\frac{\mu}{\gamma \cdot \mathbf{F}}, \frac{\sigma}{\gamma \cdot \mathbf{F}})$	**DROP**$(\mathbf{N = 160})$	**DROP**$(\mathbf{z = 3})$
(0.9125, 0.4088)	0.3781	0.3650
(0.9981, 0.2993)	0.3870	0.3763
(0.7825, 0.4856)	0.3968	0.3711

3.2 Generalizing the modeling assumptions

The geometry of the cliff is robust to a range of alternative assumptions in how p, q and g are determined. In Panels 1-3 of Figure 3 we present comparative visualizations of the cliff for three illustrative variations in the assumptions that determine p, q and g. In each case the solid line plots the baseline $E(v|R)$ cliff, and the dashed line plots the relevant comparison. In each case there is a distinct unruly regime, a compliant regime, a cliff-like transition between them, and a measured DROP exceeding our threshold.[16]

[16] In each case the value of DROP is sensitive to the assumed values of the parameters involved.

In Panel 1 we alter the technology of apprehension, which determines p. Two assumptions determine the objective probability of apprehension in the computable model: (i) exactly one unit of the enforcement resource, no more and no less, is required to investigate a violation; and, (ii) if a violation is investigated the violator is apprehended with probability γ. An alternative specification assumes that the probability that a violator is apprehended is continuous in the quantity of resources, r, devoted an investigation, $\gamma \cdot (1 - 1/\epsilon^r)$, where $\epsilon > 1$ and $0 < \gamma < 1$. This probability is increasing and concave in r and bounded above by γ. Given resources R, to maximize the expected number of apprehensions we must allocate $\frac{R}{v}$ to each violation. With this allocation, the probability that any violator is apprehended is $\gamma \cdot (1 - \frac{1}{\epsilon^{R/v}})$. In Panel 1 we assume $\epsilon = 8, \gamma = 0.8$

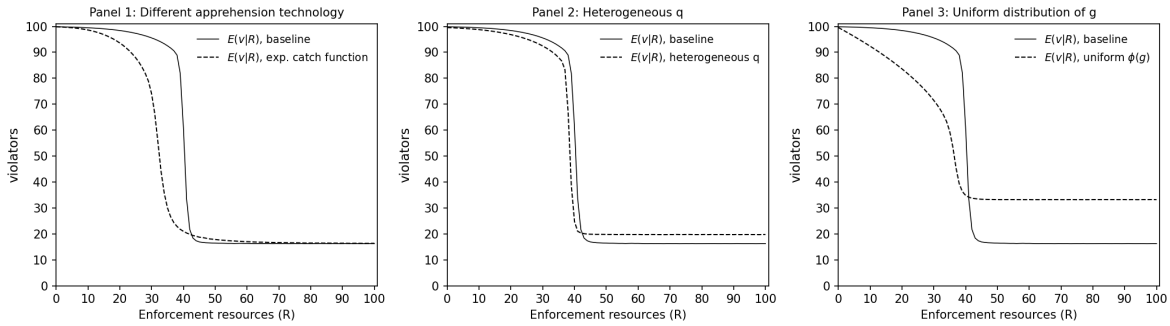

Figure 3: Robustness of the cliff, for variations in $P(v, R)$, q, and $\phi(g)$.

The code that produces Figure 3 can be found here:

- Matlab file(s): Figure 5

In Panel 2 we alter the specifications determining peoples' subjective probabilities of apprehension. The computable model assumes that all people share the same mapping from the z-history to their subjective probability of apprehension, $q_i^t = Q(zh^t) \; \forall \; i$. Alternatively, we assume $q_i^t = Q(zh^t) + \delta_i^t$, where the noise term, δ_i^t, is a person specific random draw from the uniform distribution with support $[-0.2, +0.2]$.

In Panel 3 we alter the process determining g_i^t. In the computable model, the g_i^ts are random draws from a normal distribution, $\phi(g_i^t)$. Alternatively, the g_i^ts are drawn from a uniform distribution with support $[0.2, 1.1]$.

3.3 The space of history independent policies

Another issue concerns the robustness of our results to alternative levels of sanction. In the passive policies considered in the paper the sanction F was fixed, and R varied. We now examine passive policies in which both R and F vary. We restrict our attention to passive policies for which $R \in \{0, ..., N\}$ and $F \in \{0, 0.05, ..., 1.45, 1.5\}$. This results in a set of passive polices with $101 \cdot 31 = 3131$ elements. Figure 4 is a surface plot of $E(v|R, F)$ for this set of polices. Two cross-sections are highlighted. The first is produced by holding the baseline sanction constant and varying R. This reproduces the "cliff of expected violations" illustrating disruptive positive feedback. The second is produced by holding enforcement spending constant and varying F. This produces another such cliff.

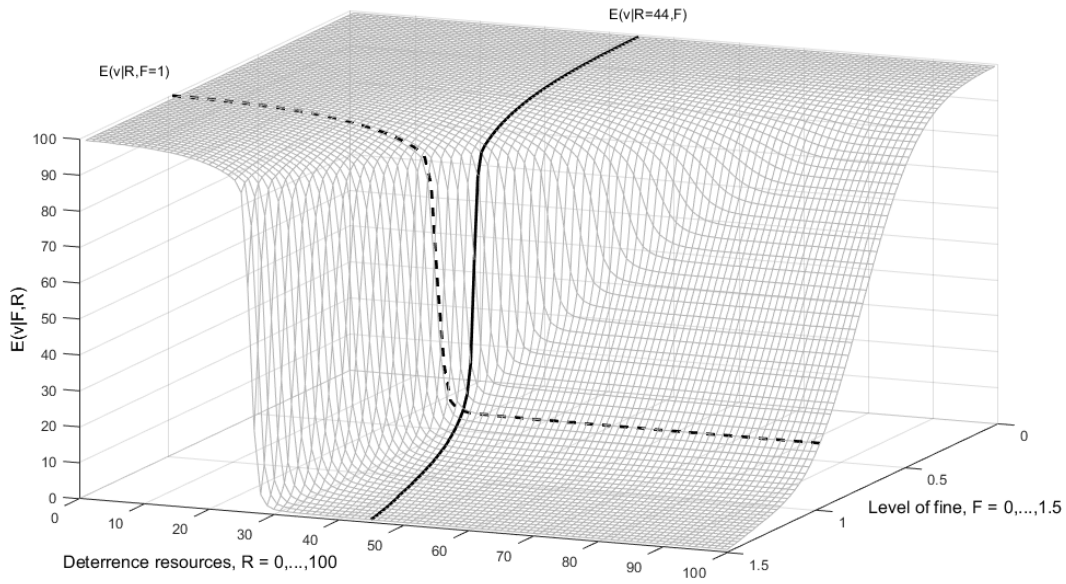

Figure 4: The space of passive policies.

The code that produces Figure 4 can be found here:

- Matlab file(s): Figure 4

Both cross-sections, as well as the surface itself, reveal the same regimes we saw in the main paper: (i) the unruly regime consists of a plateau around the top edge of the figure;

(ii) the compliant regime is the rectangular plateau at the bottom; and, (iii) the transitional regime is a cliff separating the two. The cliff in Figure 4 once again illustrates the disruptive positive feedback that occurs when the dynamic system transitions between-attractors and is a pervasive feature of our dynamic process.

3.4 The space of history dependent policies

The space of history dependent policies is much larger than that of history independent policies. Here we layout our procedure for identifying approximately optimal policies. We then demonstrate that the history dependent policies are themselves robust to the sorts of alternative assumptions we have explored to this point.

Table 7: Estimated Costs of Two-Bin Policies in the Neighborhood of the Optimum.

		BE									
		30	**31**	**32**	**33**	**34**	**35**	**36**	**37**	**38**	**39**
$\mathbf{R_1}$	**29**	131.28 **54**	130.91 **56**	130.66 **56**	130.57 **58**	130.62 **57**	130.81 **58**	131.17 **60**	131.62 **60**	132.16 **62**	132.77 **62**
	30	131.52 **55**	131.06 **55**	130.68 **56**	130.45 **57**	130.33 **56**	130.33 **57**	130.45 **59**	130.66 **60**	131.03 **61**	131.43 **62**
	31	131.97 **53**	131.11 **54**	131.11 **55**	130.76 **56**	130.52 **57**	130.37 **57**	130.35 **58**	130.41 **58**	130.58 **59**	130.82 **60**
	32	132.61 **53**	132.16 **53**	131.71 **55**	131.40 **55**	131.10 **56**	130.84 **57**	130.72 **58**	130.65 **59**	130.67 **59**	130.80 **60**

Note: The **bold** number in each cell is the associated R_2 of each policy. The standard errors for each cost estimate are in the range 0.013 to 0.017. So the deviation around each point estimate of costs in each cell is in the second decimal point (e.g. costs in the first cell range at most between 131.297 and 131.263.)

Table 7 reports the *minimum cost* of all Two-Bin history dependent policies conditioned on v^{t-1}, in the neighbourhood of the optimal policy, $\{30 \leq BE \leq 39, 29 \leq R_1 \leq 32, 53 \leq R_2 \leq 65\}$.[17] The minimization is done with respect to R_2, whose value is reported in the associated cell. For example, the upper- left cell indicates that the minimum costs of Two-Bin policies in which $(BE, R_1) = (30, 29)$ is \$131.28, and the cost minimizing R_2 is 54. As the standard errors of these estimates are all very small (i.e., $\leq$ \$0.017), it is clear that

[17] We do not produce the the table for history dependent policies conditioned on $(1 - AR^t)$, but it is a straight forward exercise and produces similar results.

the optimal policy is either $(35, 30, 57)$ or $(34, 30, 56)$. Every other cost estimate is more than 2 standard errors higher than \$130.33. Figure 5 reveals how flat costs are in this neighbourhood. The lowest cost reported in the table is \$130.80 and the highest is \$132.77, a difference of just 1.5%. It is even flatter in the R_2 dimension (not presented in the table, but shown in Panel 3 of Figure 5). For example, the cost estimate for policy (39, 31, 60) is \$130.82, and the cost estimates for four related policies, (39,31,57), (39,31,58), (30,31,59) and (30,31,61), are all within one standard error of \$130.82.

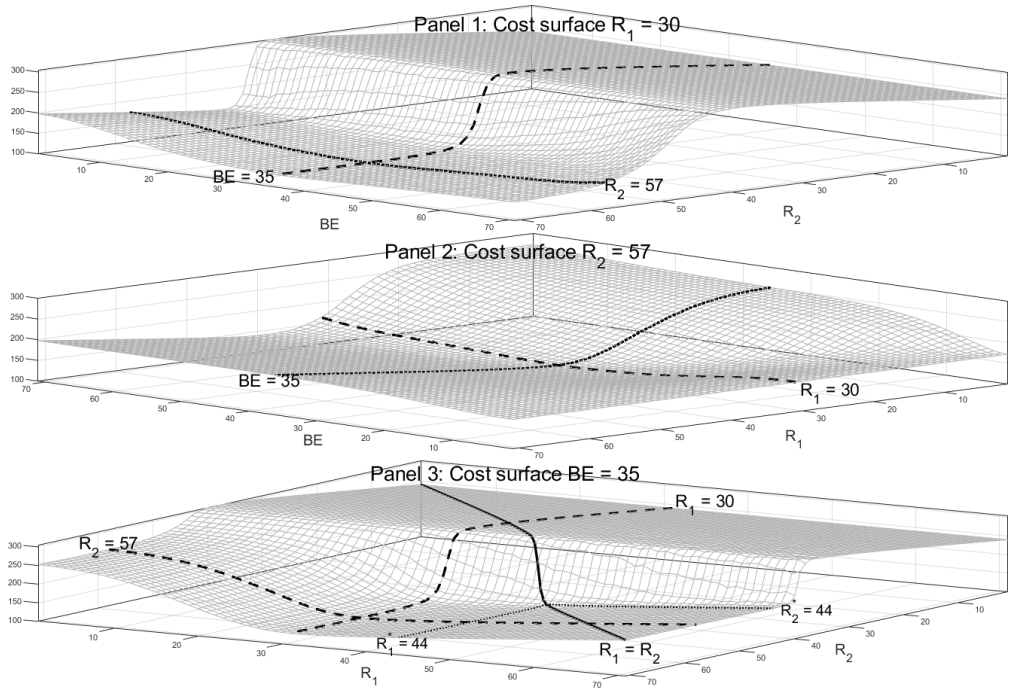

Figure 5: Surface plots of costs in BE, R_1, R_2 space

The code that produces Figure 5 can be found here:

- Matlab file(s): Figure 5

Table 8 reports results for the Three-Bin history dependent policy searches and Monte Carlo simulations for the best 25 such policies. The first two elements for a Three-Bin history dependent policy, BE_1 and R_1, are the same as those for the first two elements of one of the Two-Bin history dependent policies in the neighborhood of the optimum reported in Table 7. This reflects the fact that the search algorithm finds the same $BE = BE_1$ with

the same R_1 for the one of the Two-Bin history dependent policy policies as the Three-Bin history dependent policy. Effectively B_2, of the Two-Bin policy is partitioned into two bins, B_2 and B_3, with different quantities of the enforcement resource in the Three-Bin history dependent policy. The 25 least costly Three-Bin history dependent policies we identify in stage 1 of our search procedure are in fact refinements of one of the least costly Two-Bin policies we identified in the previous section, and presented in Table 7. Key results for the 25 Three-Bin history dependent policies with the lowest tight cost estimates are reported in Table 8. Notice that the skeletons of Tables 7 and 8 are identical.

Table 8: The Value of Refinement.

		BE									
		30	**31**	**32**	**33**	**34**	**35**	**36**	**37**	**38**	**39**
	29	1.07 9,18	0.73 11	0.62 6	XXX	XXX	XXX	XXX	XXX	XXX	XXX
R_1	**30**	XXX	XXX	0.68 2,7,15	0.49 3,4,10	0.42 1,5,8,13,14,21,22	0.17 20	XXX	XXX	XXX	XXX
	31	XXX	XXX	XXX	0.55 17	0.42 12,24	0.20 19,25	0.24 16,23	XXX	XXX	XXX
	32	XXX	XXX	XXX	XXX	XXX	XXX	XXX	XXX	XXX	XXX

All 25 of the best Three-Bin history dependent policies appear in just 11 of the 40 cells in Table 8, and 13 of them are in cells (32, 30), (33, 30) and (34, 30). In the top line of each cell we have listed the percentage difference in cost between the best Three-Bin history dependent policy and Two-Bin history dependent policy policy for that cell (from Table 7). The second line of each cell identifies the Three-Bin history dependent policy by its rank—with rank 1 being the lowest cost estimate. Policies 1, 5, 8, 13, 14, 21 and 22 are listed in cell (34, 30). All are refinements of the Two-Bin history dependent policy (34, 30, 56) from Table 7, and all produce a lower cost. This is not surprising—with more instruments to control ASB we expect to see a lower cost of ASB. What may be surprising is that the reduction in cost is relatively small—that is what the entry in the first line of each cell addresses. The cost estimate for the Three-Bin history dependent policy with rank 1 is only 0.41% lower than the costs estimate for optimal Two-Bin policy (34, 30, 56).

Table 9: Top ranked refined crackdown policies.

Rank	BE_1	BE_2	R_1	R_2	R_3	Cost	Std Error
#1	34	44	30	47	64	129.79	0.013
#2	32	37	30	42	60	129.79	0.013
#3	33	43	30	49	64	129.82	0.015

In Table 9 we report the Three-Bin history dependent policies that are ranked 1, 2 and 3, our costs estimates for them, and the standard errors of the cost estimates. When we look at the policies themselves we see that the refinements make intuitive sense. The lowest cost Three-Bin history dependent policy is $(BE_1, BE_2, R_1, R_2, R_3) = (34, 44, 30, 47, 64)$ and it is a refinement of Two-Bin policy $(BE, R_1, R_2) = (34, 30, 56)$. When Two-Bin policy $(34, 30, 56)$ is used, 56 units of enforcement resource are deployed in the B_2, $\{v^{t-1}|34 < v^{t-1} \leq 100\}$. When Three-Bin policy $(34, 44, 30, 47, 64)$ is used, B_2 from the Two-Bin policy is partitioned into B_2 and B_3 of the Three-Bin policy, $B-2$ is $\{v^{t-1}|34 < v^{t-1} \leq 44\}$ and $B-3$ is $\{v^{t-1}|44 < v^{t-1} \leq 100\}$, and quantity of enforcement resources deployed $B-2$ is 47, somewhat less 56, and quantity deployed B_3 is 64, somewhat greater than 56. When the system is in B_2 of the Two-Bin policy, the proximate objective of policy is to drive violations down and back into GA, and it makes intuitive sense that the quantity of resources needed to do that efficiently in the Three-Bin policy is smaller when violations are close to the lower bound of BA than when violations are close to the upper bound.

In Section 4.3 of the paper, to identify the optimal Two-Bin history dependent policy, we generated a tight cost estimate for every policy in the neighborhood that we identified using the stage one directed search routine. That approach is not feasible for Three-Bin history dependent policies. We can use the directed search routine to identify the neighborhood of the optimum, but there are so many policies in that neighborhood that it is not feasible to generate a tight cost estimate for each of them. In addition, in three of the five relevant dimensions, BE_2, R_2 and R_3 , the cost function is so flat that it would take thousands of convergence simulations to get cost estimates that would allow us to identify the optimal

policy.[18]

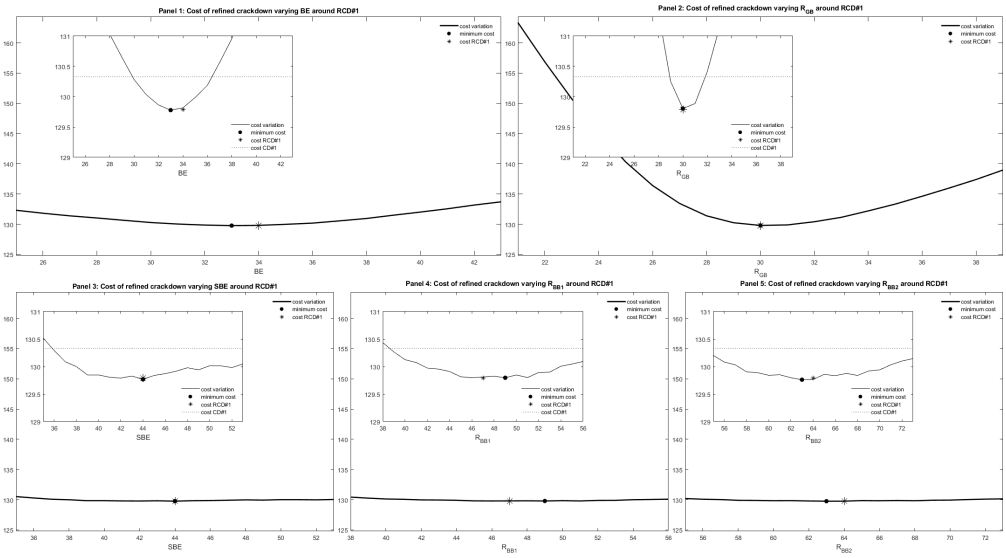

Figure 6: Cross sections of costs in the neighborhood of $Three - Bin\#1$

Nevertheless, the results reported in Figure 6 suggest that the cost of ASB for the optimal policy is very close to the cost estimates in Table 9. The cost estimates reported in the figure are based on 50 independent convergence simulations for each policy examined (the standard errors of these estimates are roughly 0.03). In each panel, cost estimates are reported for 19 policies centered on policy #1: four of the five parameters of the policy are fixed at their values in policy #1, and the fifth varies up and down from its value in policy #1 by 9 units. The asterisk indicates policy #1, and the dot the policy with the lowest cost estimate. There is considerable curvature in the cost function when R_1 and BE_1 vary, which means that the optimal values of these parameters are much easier to pin down, and that is exactly what we saw in Table 9. But over the range of values examined for parameters BE_2, R_2 and R_3, the cost function is very flat and it is much more difficult to pin down the optimal values of theses parameters. This flatness reflects the fact that there are many ways to extinguish BA, and, it does matter much in terms of costs precisely how that is achieved because so little time is spent there. The inserts in each panel present the same information but the

[18]This discussion is illustrated using history dependent policy policies conditioned on v^{t-1} but extends to history dependent policy policies conditioned on $1 - AR^t$

scale on the vertical axis is different. The more fine grained scale allows us to see how the cost estimates for the Three-Bin history dependent policies compare to our best estimate of the minimum cost achievable with the simpler Two-Bin policy—the dotted reference line in each insert represents that cost.

The code that produces Figure 6 can be found here:

- Matlab file(s): Figure 6

3.5 Generality of deterrence policy analysis

In this section we start by considering the generality and determinants of three central results for the baseline parameterization: (i) The reserve capacity rate with the optimal Two-Bin history dependent policy is higher than 60%, meaning that in a typical period only 40% of available enforcement resources are used to investigate violations; (ii) replacing the optimal history independent policy with the optimal Two-Bin, history dependent policy reduces the expected cost of ASB by 12% – 21% depending on the conditioning variable used; and, (iii) replacing the optimal Two-Bin history dependent policy policy with the optimal Three-Bin policy reduces the expected cost of ASB by less than 1% or not at all. Naturally, these specific results, the reserve capacity rate and the measured reduction in costs, will differ from one parameterization to another. We show that they are driven primarily by two factors. First, it is in part driven by the value of $DROP$ (3.1). Second, it is in part driven by the price of one unit of the enforcement resource, ρ, relative to the net external cost that violations impose on society, $(\lambda - 1)$, or what we call $RAT = (\lambda - 1)/\rho$.

As we have seen, managing ASB means managing subjective probabilities via the q-attractors by choice of R in each period. By eliminating BA, cost effective policies eliminate the disruptive positive feedback observed when the system transitions between the q-attractors. Since $DROP$ is a measure of the potential for disruptive feedback from transitioning between the q-attractors, it is intuitive that it too is important to understanding these results.

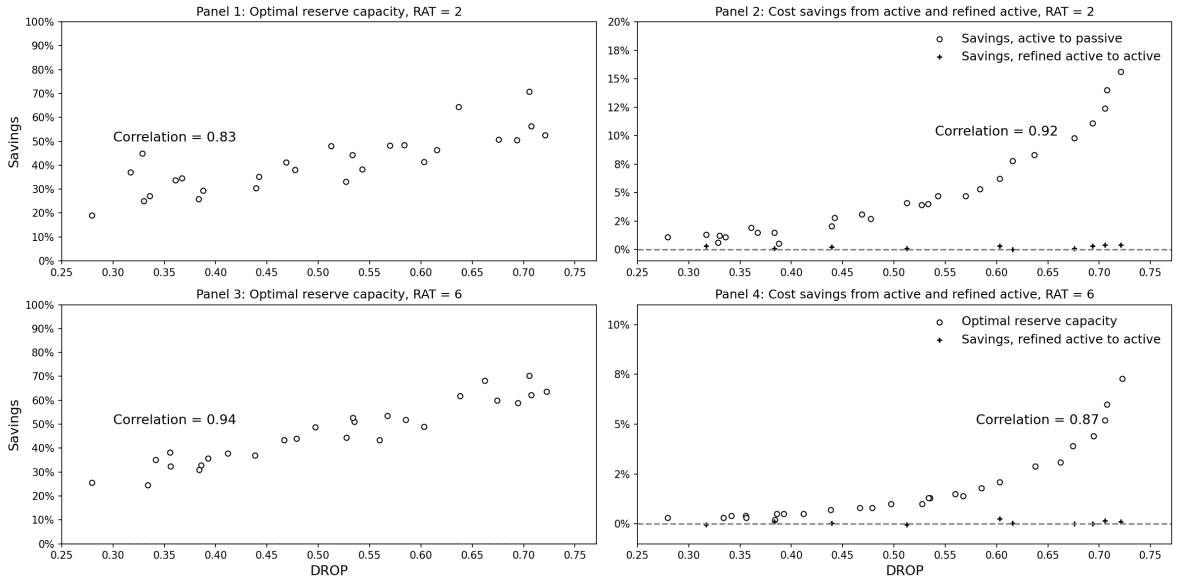

Figure 7: Reserve capacity and cost savings as a function of $DROP$.

In Figures 7 and 8 we report the reserve capacity rate and the two cost reduction percentages for simulations in which N and z are fixed at their baseline values.[19] In these figures we are treating $DROP$ as something like a composite parameter. Given $N = 100$ and $z = 2$, as we saw in Section 3, $DROP$ is determined by $\frac{\mu}{\gamma \cdot F}$ and $\frac{\sigma}{\gamma \cdot F}$. In selecting the parameterizations used in constructing these figures, we used two criteria. First, that the distribution of $DROP$ be approximately uniform over the interval (0.275, 0.725). Second, subject to this constraint, that we include parameterizations distributed across the entire $(\frac{\mu}{\gamma \cdot F}, \frac{\sigma}{\gamma \cdot F})$ parameter space. For each parameterization we calculated reserve capacity and the two cost reduction numbers. Then, in Figures 7 and 8, we plot the values for our three central results for each parameterization with their values of $DROP$ and RAT.

The first thing to notice is the magnitude of the correlation coefficients reported in the four panels of Figure 7. The fact that they are relatively high is telling us that $DROP$ does function as a composite of the parameters that determine it, and the fact they are not 1 is

[19] The estimates of optimal Two-Bin and Three-Bin history dependent policies reported in this section are generated using simpler versions of the directed search algorithms. The number of randomly seeded searches was reduced to 50 in each case implying that the errors in the estimation of the optimal policy will be slightly higher. But as we have observed, the space in which the optimum occurs is very flat and so there is very little difference between estimates in the neighborhood of the optimum. Reducing the number of searches increased computational efficiency at nearly zero cost to estimation precision.

telling us that the effects of variation in these parameters are not completely captured by $DROP$.

In Panels 1 and 3 of Figure 7, we report the reserve capacity rate for the optimal Two-Bin history dependent policy conditioned on v^{t-1} for a number of DROP values in the interval (0.25, 0.75). In Panel 1, RAT is fixed at 2 and in 3 it is fixed at 6. In both panels, reserve capacity is increasing in $DROP$, from a low of 20% up to high of 70%. In Panels 2 and 4 the circles represent the reduction in cost when the optimal passive policy is replaced with the optimal history dependent policy. In Panel 2 RAT is 2, and in 4 it is 6. The cost reduction numbers are positively associated with $DROP$ and negatively associated with RAT. The crosses in those panels represent the reduction in cost when the optimal Two-Bin history dependent policy is replaced with the optimal Three-Bin history dependent policy. These cost reduction numbers are negligible and uncorrelated with $DROP$.

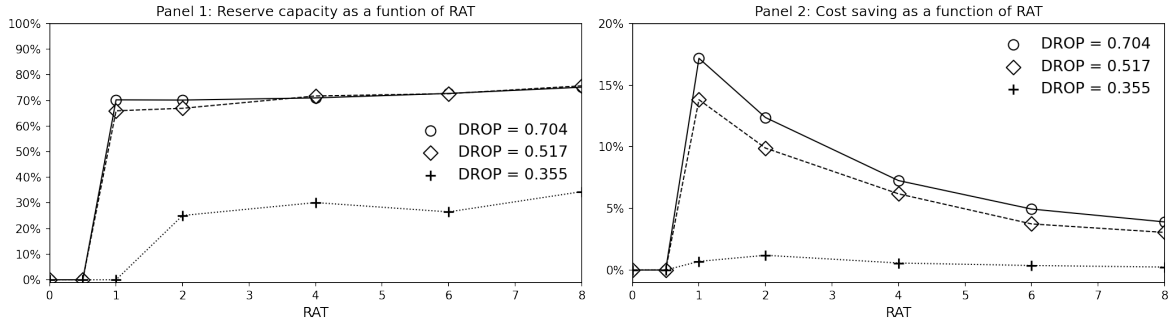

Figure 8: Reserve capacity and cost savings as a function of RAT.

In Panel 1 of Figure 8, we report the reserve capacity rate with the optimal Two-Bin history dependent policy conditioned on v^{t-1} as a function of RAT for three $DROP$ values. For all three values, there is massive discontinuity in the relationship between reserve capacity and RAT. (Given the coarse grid of RAT values, we have not identified any of the three discontinuities precisely.) When RAT is very small, we are in the spitting on the sidewalk case and the best enforcement policy is to do nothing. As RAT passes through the point of discontinuity the reserve capacity rate jumps up, and beyond the discontinuity it increases slowly with RAT. For the two larger $DROP$ values to the right of the discontinuity the

rate exceeds 60% and for the lowest value it is much lower. In Panel 2, we report the reduction in cost when the optimal history independent policy is replaced with the optimal Two-Bin history dependent policy as a function of RAT for the same three values of $DROP$. Again there is massive discontinuity in the relationship. When RAT is small do nothing is the optimal enforcement policy regardless of whether we are using a history independent or history dependent policy, so the cost reduction is 0. Beyond the discontinuity the cost reduction is inversely related to RAT.

The results reported in Figures 7 and 8 are based on parameterizations in which $N = 100$ and $z = 2$. Because simulations with larger values of these parameters are very time intensive, we have run just a few of them. Based on those simulations it seems clear that the patterns seen in these figures and the magnitudes of the numbers are robust to increases in the values of the parameters.[20]

The code that produces Figure 7 can be found here:

- Matlab file(s): Figure 7

The code that produces Figure 8 can be found here:

- Matlab file(s): Figure 8

[20] Variations of $N = 160$ and $z = 3$ were run on two values each of $DROP \approx \{0.7, 0.4\}$ and $RAT = \{2, 10\}$. The pattern of cost savings for Two-Bin and Three-Bin history dependent policies was preserved. Costs savings for Two-Bin history dependent over history independent policies increased slightly for both the larger N and z values, with the increases ranging from 0.1% to 1.8% over the baseline values with the maximum cost savings being 15.2%. The cost savings for Three-Bin history dependent was again negligible with the total savings ranging from 0% to 0.4%. The reserve capacity values were almost identical for each for each of the four cases. For example, for $DROP \approx 0.7$ and $RAT = 2$, reserve capacity = (0.4260, 0.4240, 0.4302) for the (N, z) tuples of (100, 2) (160, 2) and (100, 3) respectively.

4 Computational tools

In this section we layout some of the most important core computational tools used in analyzing the D-model.

4.1 Benchmarking the simulator

Initiating a simulation requires values for: the quantity of enforcement resources (R); people's look back horizon (z); the number of potential violators (N); the mean (μ) and standard deviation (σ) of the PDF from which each persons private gain from committing a violation is drawn $\phi(g)$; the probability a violator is apprehended if investigated (γ); the utility penalty paid by apprehended violators (F); and, the population's Bayesian priors regarding apprehension (α, β). Unless noted, we set these parameters according to our baseline parameterization in both codebases.

Given the number of states in $\boldsymbol{Z}$ for $z = 1$, it is only manageable to calculate $\boldsymbol{T}$ for $N \leq 50$. Doing so allows us to directly compute $\boldsymbol{D}$. But for $z > 1$ and larger N we must use numerical simulation methods to estimate $\boldsymbol{D}$. We benchmark our simulated estimates of $\boldsymbol{D}$ by ensuring they replicate $\boldsymbol{T}$ for the manageable set of parameters.

For each step of the simulation:

- Each potential violator is assigned a $g_i^t, \forall i \in N$ drawn randomly from $\phi(g)$ with $\mu = 0.6$ and $\sigma = 0.2$.
- A common subjective probability of apprehension, q, is calculated using the history of violations and apprehensions, $q_i^t = \frac{\alpha + a^{t-z} + \ldots + a^{t-1}}{\beta + v^{t-z} + \ldots + v^{t-1}}$, where $\alpha = 1$, $\beta = 0.25$ and for $z = 1$, $q_i^t = \frac{\alpha + a^{t-1}}{\beta + v^{t-1}}$.
- People choose to violate if and only if their $g_i^t \geq q^t \cdot F$, where $F = 1$.
- Violators are apprehended with probability $P(R^t, v^t) = p^t = \gamma \cdot \min(1, \frac{R^t}{v^t})$, where v^t is the number of violators in the current period and $\gamma = 0.8$.

- The number of violations, apprehensions, and the sum of the gains from violating (i.e., the sum of the realized draws on $\phi(g)$ for those who violated) are recorded.
- The frequency distribution of violations and apprehensions is calculated for the current period and recorded.
- The history is updated and the simulation moves to the next period.

We calculate the frequency distribution of violations and apprehensions. The frequency distribution of violations is $\boldsymbol{FV}(nv_0^t, nv_1^t, \ldots, nv_N^t)$, where nv_j^t is the number of instances in the first t periods of the simulation in which there were exactly j violations. The frequency distribution of apprehensions is $\boldsymbol{FA}(na_0^t, na_1^t, \ldots, na_N^t)$, where na_j^t is the number of instances in the first t periods of the simulation in which there were exactly j apprehensions.

The simulation proceeds in blocks of $50,000$ ticks. At the end of each block n we use $\boldsymbol{FV}$ to calculate the relative frequency distribution of violations $\boldsymbol{RFV}^n = (rv_0^n, \ldots, rv_N^n)$, where rv_j^n is the proportion of periods in which there were exactly j violations in the first $50000 \cdot n$ periods of the simulation. As n approaches infinity $\boldsymbol{RFV}^n$ approaches $\boldsymbol{D}$. The question is: How large must n be to ensure that $\boldsymbol{RFV}^n$ is a *good* estimate of $\boldsymbol{D}$? To answer this we need a convergence criterion.

At the end of each simulation block, for all $n \geq 2$, we calculate the following test statistic:

$$TEST^n = \sum_{j=0}^{j=N} |rv_j^n - rv_j^{n-1}|$$

$TEST^n$ is a measure, decreasing in n, of the *distance* between $\boldsymbol{RFV}^n$ and $\boldsymbol{RFV}^{n-1}$. $TEST^n$ does not decline monotonically, which complicates any test of convergence. After extensive experimentation we settled on the following criterion: we require that $TEST^n \leq 0.01$ for 5 consecutive blocks of n. Denoting the minimum n for which the convergence criterion is satisfied by n^* yields our approximation of the stationary distribution, $\boldsymbol{RFV}^{n^*} \sim \boldsymbol{D}$.[21]

[21] An important confounding issue for finding n^* is that the *shape* of $\boldsymbol{D}$ changes dramatically as R changes. For low values of R, $\boldsymbol{D}$ is unimodal and right skewed, for high values unimodal and left skewed,

Our convergence simulator has some limitations over certain ranges of some key parameter values, in particular those that comprise the composite parameter $\frac{\sigma}{(\gamma \cdot F)}$ defined and analyzed in Section 3.1 of this appendix. If $\frac{\sigma}{(\gamma \cdot F)}$ is small the n required to achieve a good approximation of the stationary distribution is actually much larger than the n^* generated from the convergence criteria. This is because of the persistence of the q-attractors. For these parameterizations the simulator is highly sensitive to initial conditions, staying for a very long time (sometimes the entire simulation) in only one of the q-attractors and rarely (if ever for some convergence simulations around the cliff) transitioning to the other q-attractor, even though the stationary distribution is bi-model in these parameter values. This yields a poor estimate of the stationary distribution even though the convergence simulator may have taken a very long time to converge. More accurate estimations of the stationary distribution for such parameter values would take orders of magnitude longer, longer than is feasible to make simulation useful. It is important to note that this is not a limitation of the model, but rather of our computational simulation capabilities.

Code for benchmarking of the simulator can be found at:

- Python file(s): Simulator.ipynb
- Matlab file(s): ASB BenchSD, ASB BenchTMSD,

We employ Monte Carlo simulations and the relationship between $\boldsymbol{D}$ and $\boldsymbol{RFV}^{n^*}$ to: (i) cross validate the output from our Python and Matlab codebases; and, (ii) benchmark the accuracy of the simulator against a known transition matrix.[22] The computational intensity of producing both $\boldsymbol{D}$ and $\boldsymbol{RFV}^{n^*}$ increases geometrically with the size of the state space. It is only practical, therefore, to implement both approaches for a relatively small number of agents ($N = 50$) and a single period ($z = 1$) in the history of violations and apprehensions. For these parameters, and for each element of $R = \{5, 21, 45\}$, we generate 1000 instances

for intermediate values it becomes bimodal. This renders n^* non-monotonic in R (see the last row of Table A.1).

[22] We are, of course, implicitly testing the validity of our convergence criterion.

of $\boldsymbol{RFV}^{n^*}$. We then construct the following distance metric:

$$ATEST = \boldsymbol{D} - \boldsymbol{RFV}^{n^*} = \sum_{j=0}^{j=N} |d_j - rv_j^{n^*}|$$

In Table 10 we report the mean, standard deviation, and maximal value of $ATEST$ along with the mean n^*. It is apparent that the two platforms deliver results that are essentially the same, and that $\boldsymbol{RFV}^{n^*}$ very closely approximates $\boldsymbol{D}$ as $n \to 300000$.

Table 10: Benchmarking the simulator

	Matlab Codebase			Python Codebase		
	Value of R					
	5	**21**	**45**	**5**	**21**	**45**
Mean of ATEST	0.0017	0.0098	0.0078	0.0018	0.0115	0.0087
Std Dev of ATEST	0.0009	0.0017	0.0011	0.0009	0.0019	0.0011
Max value ATEST	0.0061	0.0193	0.0116	0.0057	0.0198	0.0128
Mean n^*	6.0010	7.8430	7.0870	6.0010	7.8120	6.0010

4.2 Search algorithm for history dependent policies

We use a two stage procedure to identify the optimal Two-Bin and Three-Bin history dependent policies. In the first stage, we use a directed search routine with a loose convergence criterion to identify the neighborhood in which the optimal policy lies, and in the second stage we use Monte Carlo methods to generate tight estimates of the cost of policies in the neighborhood.

The algorithm at the core of the directed search routine is this. For a given Two-Bin history dependent policy at stage s, $CD^s = (BE^s, R_1^s, R_2^s)$, a modified policy $CD^{s+1} = (BE^{s+1}, R_1^{s+1}, R_2^{s+1})$, is generated using a three step procedure: in the first step, BE^{s+1} is chosen from the set $BE^s - 5, BE^s - 4, \ldots, BE^s + 5\}$ to minimize the cost of ASB for policy (BE^{s+1}, R_1^s, R_2^s); in the second step, R_1^{s+1} is chosen from the set $\{R_1^s - 5, R_1^s - 4, \ldots, R_1^s + 5\}$ to minimize the cost of ASB for policy $(BE^{s+1}, R_1^{s+1}, R_2^s)$; in the third step, R_2^{s+1} is

chosen from the set $\{R_2^s - 5, R_2^s - 4, \ldots, R_2^s + 5\}$ to minimize the cost of ASB for policy $(BE^{s+1}, R_1^{s+1}, R_2^{s+1})$. For each of the 33 policies considered, we ran a convergence simulation and used it to estimate cost. The search is terminated when the criteria $(E(C|CD^s) - E(C|CD^{s+1}))/E(C|CD^s) < .02$ is met. Each of the 1000 simulations was seeded with an initial policy randomly chosen from the set $\{(BE, R_1, R_2)|0 \leq BE \leq 100, 0 \leq R_1 \leq 100, R_1 \leq R_2 \leq 100\}$ and for each we used the directed search algorithm to a generate a terminal policy. From initial policy to terminal policy, the average number of policies evaluated was 165. To identify the neighborhood of the optimal crackdown policy, we ranked the 1000 terminal policies from lowest to highest cost. The first 78 policies in this ranking, and 98 of the first 100, were in the set $\{(BE, R_1, R_2)|30 \leq BE \leq 39, 29 \leq R_1 \leq 32, 53 \leq R_2 \leq 65\}$. This is neighborhood of the optimal policy.

The search for the optimal Three-Bin history dependent policy was analogous to that for the Two-Bin history dependent policy policy, with the differences being the need for two additional steps in the procedure to search over the two additional parameters, BE_2 and R_3, of the Three-Bin history dependent policy. The algorithm for the Three-Bin history dependent policy search is, given a Three-Bin history dependent policy at stage s, $CD^s = (BE_1^s, BE_2^s, R_1^s, R_2^s, R_3^s)$, a modified policy $CD^{s+1} = (BE_1^{s+1}, BE_2^{s+1}, R_1^{s+1}, R_2^{s+1}, R_3^{s+1})$, is generated using a five step procedure analogous to that of the three step procedure of the history dependent policy policy search. For each of the 55 policies considered, we again ran a convergence simulation and used it to estimate the cost. The termination criteria for the Three-Bin history dependent policy search was the same as that used for the Two-Bin policy search. The 1000 simulations were randomly seeded with initial refined crackdown policies chosen from the set $\{(BE_1, BE_2, R_1, R_2, R_3)|0 \leq BE_1 \leq 100, BE_1 \leq BE_2 \leq 100, 0 \leq R_1 \leq 100, R_1 \leq R_2 \leq R_3, R_2 \leq R_3 \leq 100\}$. From initial policy to terminal policy, the average number of policies evaluated was 440 for each of the 1000 simulations. The neighborhood of the optimal Three-Bin history dependent policy was determined in the same way as for the Two-Bin policy.

The estimate of cost that comes out of one convergence simulation is, obviously, a random variable. In the neighborhood of the optimal policy, the cost function is so flat that in order to reliably identify the optimum policy, many independent cost estimates are needed. Accordingly, for every policy in the neighborhood of the optimum we ran 150 convergence simulations and calculated the cost of ASB in the steady state for each of them. Our cost estimate is the mean value of these 150 cost estimates. Typically the standard deviation of cost for the 150 simulations is close to 0.20, and hence the standard error of the estimate is close to $0.016 = .2/\sqrt{150}$.

The code for the search algorithms and the Monte Carlo simulations over the set of policies in the neighborhood of the optimum can be found here:

Matlab file(s):

- Two-Bin history dependent policy policy v^{t-1}
- Two-Bin history dependent policy policy AR^t
- Three-Bin history dependent policy policy v^{t-1}
- Three-Bin history dependent policy policy AR^t
- Two-Bin history dependent policy policy Monte Carlo v^{t-1}
- Three-Bin history dependent policy policy Monte Carlo v^{t-1}

5 Replicating figures and core results

Here we layout and explain the code for replicating all of the figures in the paper.

5.1 Figures 3.1, 3.3

Figures 3.1, and 3.3 plot a random sample of 5000 periods of violations for the D and S-models.

Code for producing Figures 3.1, and 3.3 from Section 3 can be found here:

- Python file(s): Figures 3.1, 3.3
- Matlab file(s): Figure 3.1 Figures 3.3

5.2 Figure 3.2

Figure 3.2 plots the number, and type, of equilibria (when we assume $p^t = q^t \ \forall \ t$) as a function of R using Proposition 3.

Code for producing Figure 3.2 from Section 3 can be found here:

- Python file(s): Figure 3.2
- Matlab file(s): Figure 3.2

5.3 Figure 3.5

Figure 3.5 plots the expected number of violations for each of the three models as a function of R.

Code for producing Figure 3.5 from Section 3 can be found here:

- Python file(s): Figure 3.5
- Matlab file(s): Figure 3.5

5.4 Figure 3.6

Figure 3.6 plots a number of indices relevant to the dynamics of ASB for each of the three models as a function of R.

Code for producing Figure 3.6 from Section 3 can be found here:

- Python file(s): Figure 3.6
- Matlab file(s): Figure 3.6

5.5 Figure 3.7

Figure 3.7 plots $E(v^{t+1}|v^t)$ for $R = 39$, revealing the two q-attractors and the resulting BE.

Code for producing Figure 3.7 from Section 3 can be found here:

- Python file(s): Figure 3.7
- Matlab file(s): Figure 3.7

5.6 Figure 3.8

Figure 3.8 plots $E(v^{t+1}|v^t)$ for $R = 44$, revealing the two q-attractors and the resulting BE.

Code for producing Figure 3.8 from Section 3 can be found here:

- Python file(s): Figure 3.8
- Matlab file(s): Figure 3.8

5.7 Figure 3.9

Figure 3.9 plots measures of persistence for the q-attractors for selected values of R.

Code for producing Figure 3.9 from Section 3 can be found here:

- Python file(s):
- Matlab file(s): Figure 3.9

5.8 Figure 4.1

Figure 4.1 plots the total expected cost of managing ASB using history independent policies for all values of R for both the D and S-models.

Code for producing Figure 4.1 from Section 4 can be found here:

- Python file(s): Figure 4.1
- Matlab file(s): Figure 4.1

5.9 Figure 6.1

Figure 4.2 plots various ASB metrics illustrating the mechanics of history dependent policy policy for an arbitrarily chosen policy.

Code for producing Figure 4.2 from Section 4 can be found here:

- Python file(s): Figure 4.2
- Matlab file(s): Figure 4.2

5.10 Figure 4.3

Figure 4.3 plots $E(v^{t+1}|v^t)$ for the optimal Two-Bin history dependent policy conditioned on v^{t-1}. Panel 1 of Figure 4.3 is the plot for the optimal history dependent policy policy, $(BE, R_1, R_2) = (35, 30, 57)$ and Panel 2 is the plot of the corresponding static policy, $R = 30$.

Code for producing Figures 4.3 from Section 4 can be found here:

- Python file(s): Figure 4.3
- Matlab file(s): Figure 4.3

Figure 9 a version of Figure 4.3 from the main text, but here for the optimal Two-Bin history dependent policy conditioned on $(1 - AR^t)$ instead of V^{t-1}. Panel 1 of Figure 5 is the

plot of the optimal policy $(BE, R_1, R_2) = (0.745, 23, 48)$. Again there is just one q-attractor with focal point 17, and the frequency distribution of violations is unimodal with a mode of about 17. It is apparent that if R_2 was much less than 48 there would be two q-attractors. In Panel 2 we have constructed the q-attractor diagram for the history independent policy $(BE, R_1, R_2) = (0.745, 23, 23)$. Now there are two q-attractors with focal points 17 and 97, but again as the frequency distribution in Panel 2 indicates the persistence of BA is so much larger than that of GA that time spent in GA is vanishingly small. The policy difference between the two panels in the figure is as in Figure 4.3 of the main paper: in Panel 1 instead of deploying 23 units of enforcement resources in BA, 48 units are deployed, extinguishing BA. Comparing the frequency distributions in the two panels we see the dramatic positive consequences. As in the main text We see again: cost effectively managing the deterrence process requires eliminating BA.

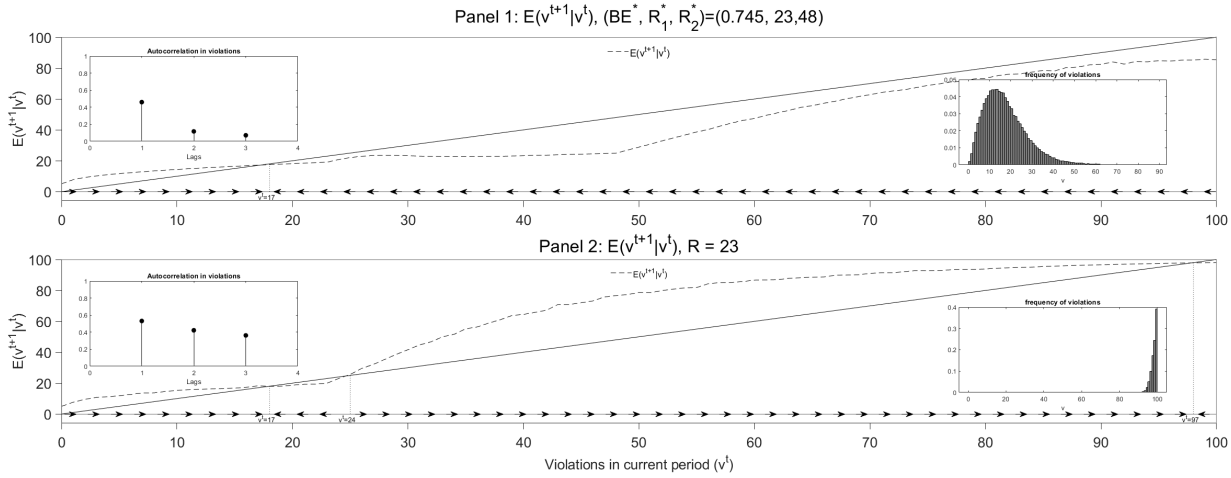

Figure 9: Extinguishing BA with a Two-Bin policy conditioned on $(1 - AR^t)$.

The code base for producing figure 9 can be found here:

- Matlab file(s): Figure 9

6 Equilibrium selection (Pareto-dominant equilibria)

In the S-model we resolve the equilibrium selection problem by choosing the equilibrium with the lowest number of violations – for convenience we call it the L-equilibrium. The fact that the aggregate utility in the L-equilibrium is larger than it is in any other equilibrium suggests that it may be salient.

Here we establish two additional results that support salience of the L-equilibrium. To establish them we assume that he external effects of violations are distributed equally across all N people.

- First result: the L-equilibrium is never Pareto-dominated by another equilibrium.
- Second result: in the baseline model the probability that the L-equilibrium Pareto-dominates all others is very close to one for every $R \in \{0, 1, ..., N\}$.

Suppose we have more than one equilibrium for some realization of the gs. Order the realizations from highest to lowest: $g_1 \geq g_2 \geq ... \geq g_N$. Denote the number of violations in the L-equilibrium by L and the number of violations in some other equilibrium by H, where $N \geq H > L \geq 1$.

The assumption that there is an equilibrium with L violations and one with H violations implies that the following inequalities hold.

$$g_L \geq p(L) * F$$

and

$$g_{L+1} < p(L+1) * F.$$

The external costs of ASB born by every person in the two equilibria are:

$$EX(L) = \frac{(\lambda - 1)}{N} * (g_1 + g_2 + ... + g_L)$$

and

$$EX(H) = \frac{(\lambda - 1)}{N} * (g_1 + g_2 + ... + g_H).$$

The difference between $EX(H)$ and $EX(L)$ is positive and equal to:

$$EX(H) - EX(L) = \frac{(\lambda - 1)}{N} * (g_{L+1} + g_{L+1} + ... + g_H) > 0.$$

To discern whether the L-equilibrium Pareto-dominates the H-equilibrium, we need to compare the utilities in the two equilibria of three groups of people. Group 1 includes all the people who choose comply in both equilibria, persons $H+1, H+2, ..., N$. The utilities of each person in two equilibria are $-EX(L)$ and $-EX(H)$. Clearly, their utility is larger in the L-equilibrium than it is in the H-equilibrium, since $EX(H) - EX(L) > 0$. This establishes the first result – the L-equilibrium is never Pareto-dominated by another equilibrium.

Group 2 includes all the people who chose comply in the L-equilibrium and violate in the H-equilibrium, persons $L + 1, L + 2, ..., H$. The utility of person K, where K satisfies $L + 1 \leq K \leq H$, is $-EX(L)$ in the L-equilibrium and $g_K * p(H) * F - EX(H)$ in the H-equilibrium. Person K's utility is greater in the L-equilibrium if $EX(H) - EX(L) > g_K - p(H) * F$. Pareto-dominance of the L-equilibrium requires that this inequality holds for everyone in Group 2. Since person $L + 1$ is the person who is least likely to satisfy the inequality, Pareto-dominance requires that $EX(H) - EX(L) > g_{L+1} - p(H) * F$ or that

$$\frac{(\lambda - 1)}{N} * (g_{L+1} + g_{L+1} + ... + g_H) > g_{L+1} - p(H) * F.$$

Notice that the larger is λ the more likely it is that this inequality will hold. This is not surprising, but mildly interesting. In the baseline model the inequality boils down to:

- Inequality A: $\frac{1}{25} * (g_{L+1} + g_{L+1} + ... + g_H) > g_{L+1} - p(H)$.

Recalling that the gs are independent draws for the normal distribution for the baseline model, it is clear the inequality may or may not be satisfied.

Group 3 includes all the people who chose violate in both equilibria, persons $1, 2, ..., L$. The utility of person K, where K now satisfies $1 \leq K \leq L$, is $g_K - p(L) * F - EX(L)$ in the L-equilibrium and $g_K - p(H) * F - EX(H)$ in the H equilibrium. Pareto-dominance of the L-equilibrium requires that the following inequality holds for everyone in Group 3:

$$EX(H) - EX(L) > F(p(L) - p(H))$$

or that

$$\frac{(\lambda - 1)}{N} * (g_{L+1} + g_{L+1} + ... + g_H) > F * (p(L) - p(H)).$$

In the baseline model the inequality is:

- Inequality B: $\frac{1}{25} * (g_{L+1} + g_{L+1} + ... + g_H) > (p(L) - p(H))$.

Once again, it is clear the inequality may or may not be satisfied depending on the random draw of the gs.

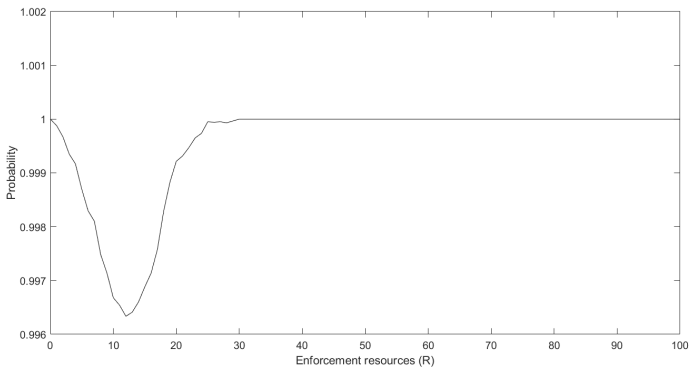

Figure 10: Probability L-equilibrium is Pareto dominant.

So far we have established that, in the baseline model, the L-equilibrium Pareto-dominates the H-equilibrium if and only if inequalities A and B hold. To establish the second result – in the baseline model the probability that the L-equilibrium Pareto-dominates all others is very close to one for all R in the set $\{0, 1, ..., N\}$ – we conducted a series of Monte Carlo experiments to estimate for each of the 101 Rs the probability that the L-equilibrium

is Pareto-dominant. For each R we generated 200,000 realizations of $(g_1, g_2, ..., g_N)$. For each realization, we found all the equilibria, and determined whether the L-equilibrium was Pareto-dominant. When there is just one equilibrium, the L-equilibrium is obviously Pareto-dominant. When there was more than one we used inequalities A and B to establish whether L-equilibrium was Pareto-dominant. In Figure 10 we report the relative frequency in these Monte Carlo experiments of cases in which the L-equilibrium was Pareto-dominant. None of the relative frequencies in the figure is less than 0.996 and for $R \geq 30$ it is equal to 1.

References

Apel, Robert, "Sanctions, Perceptions, and Crime: Implications for Criminal Deterrence," *Journal of Quantitative Criminology*, March 2013, *29* (1), 67–101.

Banerjee, Abhijit, Esther Duflo, Daniel Keniston, and Nina Singh, "The Efficient Deployment of Police Resources: Theory and New Evidence from a Randomized Drunk Driving Crackdown in India," 2019, p. 86.

Chalfin, Aaron and Justin McCrary, "Criminal Deterrence: A Review of the Literature," *Journal of Economic Literature*, 2017, *55* (1), 5–48.

Corman, Hope and H. Naci Mocan, "A Time-Series Analysis of Crime, Deterrence, and Drug Abuse in New York City," *The American Economic Review*, 2000, *90* (3), 584–604.

_ **and Naci Mocan**, "Carrots, Sticks, and Broken Windows," *The Journal of Law & Economics*, 2005, *48* (1), 235–266.

Curry, Philip A., Anindya Sen, and George Orlov, "Crime, Apprehension and Clearance Rates: Panel Data Evidence from Canadian Provinces," *The Canadian Journal of Economics / Revue canadienne d'Economique*, 2016, *49* (2), 481–514.

Fajnzylber, Pablo, Daniel Lederman, and Norman Loayza, *Determinants of Crime Rates in Latin America and the World: An Empirical Assessment*, The World Bank, October 1998.

_ **,** _ **, and** _ , "What Causes Violent Crime?," *European Economic Review*, July 2002, *46* (7), 1323–1357.

Fu, Chao and Kenneth I Wolpin, "Structural Estimation of a Becker-Ehrlich Equilibrium Model of Crime: Allocating Police Across Cities to Reduce Crime," *The Review of Economic Studies*, October 2018, *85* (4), 2097–2138.

Glaeser, Edward L., Bruce Sacerdote, and José A. Scheinkman, "Crime and Social Interactions," *The Quarterly Journal of Economics*, 1996, *111* (2), 507–548.

Greenberg, David F., "Time Series Analysis of Crime Rates," in Shawn Bushway and David Weisburd, eds., *Quantitative Methods in Criminology*, first ed., Routledge, July 2017, pp. 539–575.

Hansen, Benjamin, "Punishment and Deterrence: Evidence from Drunk Driving," *The American Economic Review*, 2015, *105* (4), 1581–1617.

Jacob, Brian, Lars Lefgren, and Enrico Moretti, "The Dynamics of Criminal Behavior: Evidence from Weather Shocks," *Journal of Human Resources*, 2007, *XLII* (3), 489–527.

Lim, Up and George Galster, "The Dynamics of Neighborhood Property Crime Rates," *The Annals of Regional Science*, December 2009, *43* (4), 925–945.

Lochner, Lance, "Individual Perceptions of the Criminal Justice System," *The American Economic Review*, 2007, *97* (1), 444–460.

Loureiro, Andre, "Asymmetric Effects and Hysteresis in Crime Rates: Evidence from the United States," 2013, p. 53.

MacDonald, John, Jeffrey Fagan, and Amanda Geller, "The Effects of Local Police Surges on Crime and Arrests in New York City," *PLOS ONE*, June 2016, *11* (6), e0157223.

Matsueda, Ross L., Derek A. Kreager, and David Huizinga, "Deterring Delinquents: A Rational Choice Model of Theft and Violence," *American Sociological Review*, February 2006, *71* (1), 95–122.

Mocan, H. Naci and Turan G. Bali, "Asymetric Crime Cycles," *The Review of Economics and Statistics*, 2010, *92* (4), 899–911.

Nagin, Daniel S., "Deterrence: A Review of the Evidence by a Criminologist for Economists," *Annual Review of Economics*, August 2013, *5* (1), 83–105.

Perc, Matjaž, Karsten Donnay, and Dirk Helbing, "Understanding Recurrent Crime as System-Immanent Collective Behavior," *PLoS ONE*, October 2013, *8* (10), e76063.

Poutvaara, Panu and Mikael Priks, "Hooliganism in the Shadow of the 9/11 Terrorist Attack and the Tsunami: Do Police Reduce Group Violence?," CESifo Working Paper Series 1882, CESifo 2006.

Ratcliffe, Jerry H., Elizabeth R. Groff, Evan T. Sorg, and Cory P. Haberman, "Citizens' Reactions to Hot Spots Policing: Impacts on Perceptions of Crime, Disorder, Safety and Police," *Journal of Experimental Criminology*, September 2015, *11* (3), 393–417.

Sah, Raaj K., "Social Osmosis and Patterns of Crime," *Journal of Political Economy*, 1991, *99* (6), 1272–1295.

Sherman, Lawrence W., "Police Crackdowns: Initial and Residual Deterrence," *Crime and Justice*, 1990, *12*, 1–48.

Weisburd, Sarit, "Police Presence, Rapid Response Rates, and Crime Prevention," *The Review of Economics and Statistics*, May 2021, *103* (2), 280–293.

Worrall, John L and Travis C Pratt, "Estimation Issues Associated with Time-Series—Cross-Section Analysis in Criminology," 2004.